Regions of Interest–Based Discriminant Analysis of DaTSCAN SPECT and FDG-PET for the Classification of Dementia

Valentina Garibotto, MD,† Marie Louise Montandon, PhD,* Claire Tabouret Viaud, MD,* Mohamed Allaoua, MD,* Frédéric Assal, MD,†‡ Pierre R. Burkhard, MD,†‡ Osman Ratib, MD,*† and Habib Zaidi, PhD*†§*

Purpose: Neuroimaging is increasingly used to support the clinical diagnosis of patients with cognitive impairment. Dopamine transporter (DAT) imaging, such as DaTSCAN SPECT, tests the integrity of the nigrostriatal pathway, whereas FDG-PET identifies typical patterns of cortical and subcortical hypometabolism. The aim of this study was to assess the relative contribution of DAT and regional glucose metabolism imaging to the differential diagnosis.

Patients and Methods: Twenty-seven subjects were investigated for neurodegenerative dementia associated with parkinsonism of variable severity by FDG-PET and DaTSCAN SPECT. They were grouped according to the clinically established diagnosis, including probable Alzheimer disease (5 subjects), corticobasal degeneration (6 subjects), Lewy body dementia (8 subjects), frontotemporal dementia (4 subjects), and Parkinson disease with dementia (4 subjects). Normalized FDG uptake and DAT uptake ratios were obtained by the BRASS software. We used a discriminant analysis with a stepwise method and a leave-one-out cross-validation.

Results: With the use of regional values of normalized FDG uptake, 85.2% and 55.6% of the patients were correctly classified by the discriminant analysis and the cross-validation, respectively. When DAT alone was considered, the results were 59.3% and 51.9%, whereas the combination of both DAT and normalized FDG uptake yielded 100% and 88.9% of accurate classifications.

Conclusions: This automated analysis approach shows that the information provided by normalized FDG uptake and DAT is not redundant for the differential diagnosis of dementia and that taking into account both normalized FDG uptake and DAT uptake allows a better classification of individual patients. These results further support the usefulness of both modalities in the clinical workup of dementia.

Key Words: brain imaging, FDG-PET, DaTSCAN SPECT, dementia, quantitative analysis

(*Clin Nucl Med* 2013;38: e112–e117)

Functional neuroimaging is increasingly used to supplement the clinical diagnosis of patients with neurodegenerative dementia and various degrees of parkinsonism because both conditions are frequently associated in clinical practice and remain a real challenge to clinicians. The most prevalent neurodegenerative conditions associating cognitive decline with parkinsonism include Alzheimer disease (AD), Lewy body dementia (LBD), Parkinson disease dementia (PDD), frontotemporal dementia (FTD), and corticobasal degeneration (CBD). Clinically, it may be difficult to establish a firm diagnosis among them, especially at an early stage. For example, suggestive features, such as visual hallucinations in PDD and LBD, may manifest only at an advanced stage or not at all.

The current status of functional neuroimaging to investigate neurodegeneration of the nigrostriatal pathway for the differential diagnosis of parkinsonism has been recently reviewed,[1] focusing mainly on dopamine transporters (DATs).[2] DaTSCAN SPECT, in particular, has been validated for differential diagnosis between LBD and non-LBD with a sensitivity and specificity of 78% and 90%, respectively.[3] Because of the variable degree of caudate nucleus involvement and a highly conserved pathologic change across the substantia nigra in Parkinson disease (PD), patterns of symmetry and caudate-to-putamen ratios can differ among groups, but presynaptic dopaminergic imaging alone does not allow accurate differentiation between PD and atypical parkinsonian syndromes.[4–6]

Imaging of brain perfusion or metabolism, on the other hand, has been used to distinguish these disorders in vivo, but most studies compared only 2 groups of specific disease entities.[7–9] One study using ^{18}F-FDG-PET and pattern recognition on individual statistical parametric maps in patients with PD, multiple-system atrophy, progressive supranuclear palsy, and CBD found that automated classification agreed with the clinical diagnosis in 92.4% of the cases.[10] However, this study did not include patients with LBD, AD, or FTD.

Thus, when the clinical picture is ambiguous, DAT imaging is performed to confirm the involvement of the nigrostriatal pathway related to parkinsonism and FDG-PET to identify typical pattern of cortical and subcortical hypometabolism associated with cognitive deficits. Some groups have described the contribution of either modality in the imaging characterization of different neurodegenerative conditions,[8,11,12] and so far, only one group investigated the added value of measuring both DAT and cortical involvement (using perfusion SPECT) in the differential diagnosis of parkinsonian disorders.[13]

The aim of this retrospective study was therefore to investigate the contribution of DaTSCAN and FDG-PET imaging to classify the patients in diagnostic groups using an operator-independent, automated template-based discriminant analysis method. As operational criterion standard, clinical diagnosis after a follow-up of at least 6 months was taken.

PATIENTS AND METHODS

Patients

We retrospectively evaluated our database of internal referrals for combined FDG-PET and DaTSCAN SPECT between 2006 and 2011. The inclusion criteria were as follows:

- To have undergone both FDG-PET and DAT imaging not more than 6 months apart, requested by the referring clinician;
- To have CT or MR morphological imaging excluding vascular lesions;
- To fulfill a diagnosis of probable AD, CBD, PDD, LBD, and FTD according to established clinical criteria.[14–18] The diagnosis was independently confirmed by 2 dementia and movement disorders specialists (F.A., P.R.B.);
- To have a minimum follow-up of 1 year, during which no diagnostic change was made;
- To be right handed.

Received for publication May 4, 2012; revision accepted September 10, 2012.
From the *Nuclear Medicine and Molecular Imaging Unit, Department of Medical Imaging, Geneva University Hospitals; †Faculty of Medicine, Geneva University; ‡Neurology Unit, Department of Clinical Neurosciences, Geneva University Hospitals, Geneva, Switzerland; and §Department of Nuclear Medicine and Molecular Imaging, University Medical Center Groningen, University of Groningen, Groningen, the Netherlands.
H.Z. was supported by the Swiss National Science Foundation under grants SNSF 31003A-135576 and 33CM30-124114. V.G. was supported by the Aetas Swiss foundation for Ageing Research.
Reprints: Valentina Garibotto, MD, Hôpitaux Universitaires de Genève, Rue Gabrielle-Perret-Gentil 4, 1211 Genève 14, Switzerland.
E-mail: valentina.garibotto@hcuge.ch.
Conflicts of interest and sources of funding: none declared.

ISSN: 0363-9762/13/3803–e112

We obtained a total of 27 patients, grouped as follows: 5 for AD, 6 for CBD, 8 for LBD, 4 for FTD, 4 for PDD. The clinical diagnosis of probable AD, CBD, PDD, LBD, and FTD was made according to established criteria. Patients' demographic data are given in Table 1 for the 5 considered groups.

This retrospective study was approved by the local ethical committee.

Data Acquisition and Reconstruction

FDG-PET

All subjects received about 250 MBq of ^{18}F-FDG in slow IV injection under standardized injection circumstances (supine, low ambient noise, dimly lit room, eyes closed). Usual medication schemes were continued before and on the day of the scan.

PET/CT data acquisition was performed on a Biograph Sensation (Siemens Healthcare, Erlangen, Germany) using a standard protocol recommended by the manufacturer. The PET acquisition was started approximately 30 minutes after injection of ^{18}F-FDG. The PET emission study (20 minutes, 1 bed position) followed immediately the CT study used for attenuation and scatter correction. Image reconstruction was performed using a filtered-back projection algorithm.

DAT SPECT

^{123}I-FP-CIT (DaTSCAN; Amersham Health–GE Healthcare) SPECT was performed within 1 month from the PET study for all but 2 patients (an interval of 8 month for 1 AD patient and of 12 months for 1 PD patient were considered acceptable). All patients received about 185 MBq of ^{123}I-FP-CIT in slow IV injection. Thyroid uptake was blocked before the scan by administration of Lugol solution (5 drops 5% KI administered before and 4 hours after injection). SPECT data acquisition started 4 hours after administration of the DAT tracer. Dopaminergic agents, whenever used, were not discontinued.

The scans were acquired on a triple-head gamma-camera (Toshiba Medical Systems, Tokyo, Japan) equipped with a fan-beam, low-energy, high-resolution collimators. In all cases, the head was fixed in a head holder to minimize motion artefacts. Acquisition parameters included step-and-shoot mode over 30 minutes. Sixty projection angles were taken over 360 degrees and a 128 × 128 matrix was used. Reconstruction was performed using filtered projection using a Shepp and Logan filter. The triple-energy window method was used for scatter compensation, whereas a uniform Chang attenuation correction was used to compensate for photon attenuation using a uniform attenuation coefficient of 0.15/cm.

Image Processing and Data Analysis

FDG-PET and DaTSCAN images were quantitatively analyzed using BRASS automated functional brain analysis software (Hermes BRASS software, Nuclear Diagnostics AB, Sweden). Briefly, BRASS fits and compares patients' images to 3-dimensional reference templates created from images of healthy subjects.[19] FDG-PET images were warped[20] individually to the BRASS template.

DAT images were also evaluated using BRASS. This analysis takes the tomographic data, spatially registers them to a template in a standard space, and finds the count concentration in striatal (Cs) and background occipital (Cb) volumes of interest. With the use of the activity concentrations in the volumes of interest (VOIs), striatal uptake ratios defined as (Cs − Cb) / Cb of specific tracer binding are calculated.

The template VOI sets were predefined in the BRASS software.[21,22]

For the analysis of FDG data, we took into account the following VOIs covering cerebral gray matter, that is, superior, middle, and inferior frontal gyrus; precentral and postcentral gyrus; paracentral lobule; superior, middle, and inferior temporal gyrus; inferior and superior parietal lobule; angular gyrus; supramarginal gyrus; superior, middle, and inferior occipital gyrus; precuneus; cuneus; uncus hippocampi; hippocampal gyrus; cingulate gyrus; thalamus; putamen; caudate nucleus.

For activity normalization, relative uptake values were determined by dividing VOI uptake by the total cerebral gray matter uptake (overall gray matter VOI), thus providing regional normalized FDG uptake values.

For DAT, uptake ratios measured for the caudate and the putamen, for the more and less affected hemisphere, relative to occipital activity, were taken as input variables.

An example of FDG-PET and DaTSCAN SPECT images in a case of AD, showing the normalized images as well as the VOI template, is provided in Figure 1.

TABLE 1. Patients' Demographic Characteristics, According to the Following Diagnostic Groups: AD, LBD, PDD, FTD, and CBD

	Age, Mean (SD), Range	Sex, Male-Female Ratio
AD	80,2 (4.9), 73–86	3:2
CBD	73 (7.2), 63–84	4:2
FTD	69.5 (6.9), 67–76	2:2
LBD	71.9 (5.1), 72–78	6:2
PDD	61 (6.7), 61–68	1:3
Total	71.7 (8)	16:11

Discriminant Analysis and General Statistics

All general statistical analyses were performed using PASW (SPSS version 18.0 for Windows; SPSS Inc). Then general discriminant modeling was used to perform the discriminant analysis.

Discriminant analysis is a statistical approach used to predict a categorical dependent variable (called a *grouping variable*) by one or more continuous or binary independent variables (called *predictor variables*). In this case, the continuous independent variables are represented by the regional DAT uptake and normalized FDG uptake values. Discriminant analysis works by creating one or more (for more than 2 groups) linear combinations of predictor variables that provide the best discrimination between the groups: these are called *discriminant functions* and have the form displayed in the Equation 1:

$$d_{\mathrm{ik}} = b_{0k} + b_{1k}x_{i1} + \ \ldots + b_{\mathrm{pk}}x_{\mathrm{ip}} \qquad (1)$$

where d_{ik} is the value of the kth discriminant function for the ith case, p is the number of predictors, b_{jk} is the value of the jth coefficient of the kth function, x_{ij} is the value of the ith case of the jth predictor.

The functions are generated from a sample of cases for which group membership is known, in our case the whole sample of subjects grouped according to clinical diagnosis.

Stepwise forward analysis was used to identify possible multiple variables for optimal discrimination, with a decision scheme based on the smallest F ratio (maximum significance of F to enter, 0.10; maximum significance of F to remove, 0.20). The a priori classification probability was set as being equal to ascertain a conservative estimate.

Classification performance was initially tested using the training error, that is, by post hoc classification statistics. To estimate a more unbiased and generalized performance measure for new patient cases, the a priori discriminant value or discriminant cross-validity was tested using a classical leave-one-out procedure.[23] In this cross-validation,

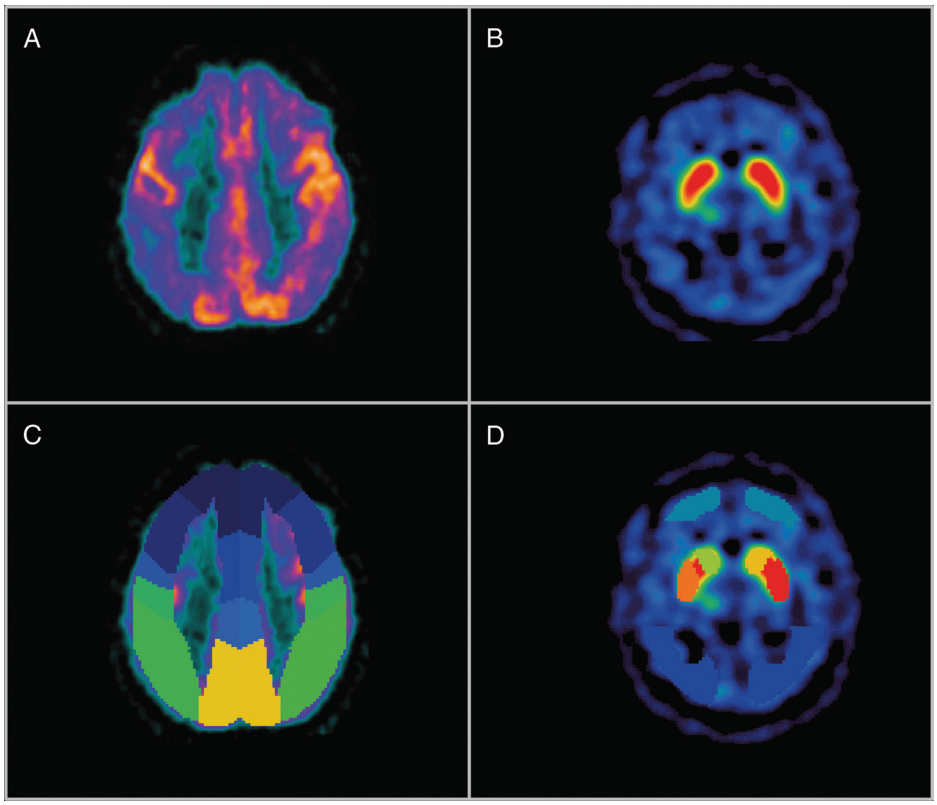

FIGURE 1. A and B, Normalized images of FDG-PET (**A**) and DaTSCAN SPECT (**B**) in a patient with a clinical diagnosis of AD and typical imaging findings: the DAT binding is within the normal range, and the glucose metabolism is reduced in the temporoparietal regions, bilaterally. **C** and **D**, Corresponding VOI maps in the BRASS software, overlaid on the normalized images.

each case is classified by the functions derived from all cases other than that case.

RESULTS

Discriminant analysis was performed for DAT and normalized FDG uptake data separately, as well as combining the 2 data sets.

DAT Values

The stepwise discriminant analysis retained the DAT uptake ratio in the most affected putamen and in the least affected caudate as significant, with 59.3% of originally grouped cases correctly classified and 51.9% of cross-validated grouped cases correctly classified. The eigenvalues, canonical correlation coefficients, and percentage of variance explained by each discriminant function are provided in Table 2. The region with the highest coefficient in the first discriminant function is the most affected putamen (1.969) and in the second discriminant function the less affected caudate (1.467). The distribution of the cases according to the 2 canonical discriminant functions is shown in Figure 2.

Regional Normalized FDG Uptake Values

The stepwise discriminant analysis retained as significant the normalized FDG uptake in the right inferior parietal lobule, in the right and left precuneus, in the right thalamus, and in the right putamen: 85.2% of the originally grouped cases were correctly classified, whereas 55.6% were correctly classified after cross-validation. The eigenvalues, canonical correlation coefficients, and percentage of variance explained by each discriminant function are provided in Table 2. The region with the highest coefficient in the first and the second discriminant function is the right precuneus (2.257 and 2.689, respectively). The distribution of the cases according to the first 2 canonical discriminant functions is shown in Figure 3.

Combined DAT and Normalized FDG Uptake Values

The stepwise discriminant analysis retained as significant the DAT uptake ratio in the most affected putamen and in the least affected caudate, as well as normalized FDG uptake in the left precentral gyrus, in the right postcentral gyrus, in the right inferior parietal lobule, in the left superior parietal lobule, in the right inferior occipital gyrus, in the left cuneus, in the left precuneus, in the right hippocampus, in the right cingulate gyrus, in the right and left thalami, and in the right putamen. By using these regional values, 100% of the original grouped cases and 88.9% of cross-validated grouped cases were correctly classified. The eigenvalues, canonical correlation coefficients, and percentage of variance explained by each discriminant function are provided in Table 2. The region with the highest coefficient in the first discriminant function is the relative FDG uptake in left precuneus (5.960) and in the second discriminant function the most affected putamen DAT binding (4.999). The distribution of the cases according to the first 2 canonical discriminant functions is shown in Figure 4.

DISCUSSION

Functional neuroimaging has become a pivotal tool in the investigation of neurodegenerative conditions, supporting clinical diagnosis and having a relevant impact on therapy selection and prognosis. In particular, molecular imaging allows individualized classification of patients based on specific biomarkers, such as the distribution of glucose metabolism and the impairment of the nigrostriatal pathway.

TABLE 2. Summary of the Results of the Discriminant Analysis Based on DAT Uptake Values, on Relative FDG Uptake Values, and on Both

Values Included in the Analysis	Function	Eigenvalue	Canonical Correlation	Percentage of Variance	Cumulative Percentage of Variance
Regional DAT values					
	1	1.919	0.811	86.6	86.6
	2	0.298	0.479	13.4	100.0
Regional normalized FDG uptake values					
	1	8.134	0.944	79.7	79.7
	2	1.224	0.742	12.0	91.7
	3	0.626	0.620	6.1	97.9
	4	0.218	0.423	2.1	100.0
Regional DAT values and normalized FDG uptake values					
	1	73.438	0.993	71.6	71.6
	2	19.382	0.975	18.9	90.4
	3	8.430	0.945	8.2	98.7
	4	1.372	0.761	1.3	100.0

The table reports the eigenvalues, the canonical correlation coefficients, the percentage of variance explained by each discriminant functions, and the cumulative percentage of variance explained by the model.

DaTSCAN SPECT and PET metabolic imaging are 2 techniques frequently used for patients referred for cognitive disturbances and some degree of parkinsonism, often early in the disease course. The patterns of DAT involvement and FDG impairment in these diagnostic entities are well known and have been described in larger samples.[6,24,25]

DaTSCAN is already known to be unable to distinguish the different causes of degenerative parkinsonism between them.[6]

However, is the metabolic/perfusion information sufficient to classify the patients in diagnostic groups?

Multitracer imaging analyzed with automated methods for differential diagnosis among these clinical entities has not been much explored yet. Only a few previous studies used an automated approach to classify patients on the basis of their imaging features: most of these studies used only one imaging modality, such as PET or perfusion SPECT, with overall good performances.[26–28] Only one previous study used the combined information of DaTSCAN SPECT and perfusion SPECT to differentiate PD, progressive supranuclear palsy, multiple-system atrophy, LBD, and essential tremor with superior results when

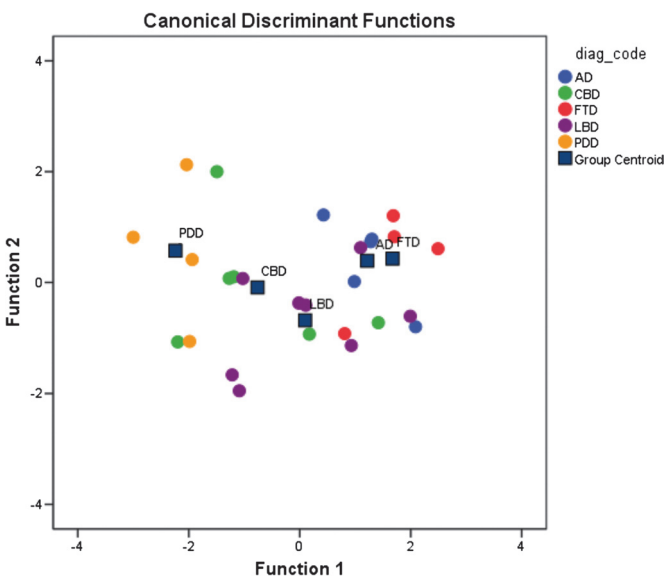

FIGURE 2. Two-dimensional projection plot of discriminant canonical functions for differentiation of patients with dementia using DAT imaging. On the *x* and *y* axes, the 2 discriminant functions, that is, the 2 linear combinations of the regional values providing the best discrimination between the groups. Colored dots indicate individual data, by clinical diagnosis, that is, AD, LBD, PDD, FTD, and CBD. The squares indicate the group centroids.

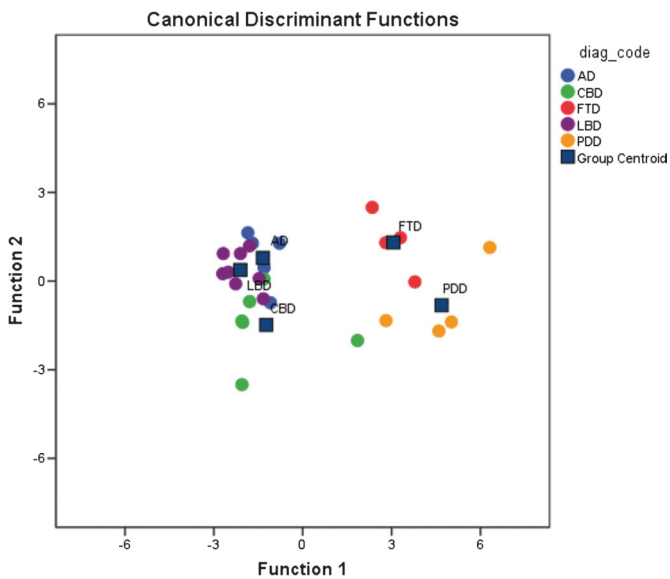

FIGURE 3. Two-dimensional projection plot of discriminant canonical functions for differentiation of patients with dementia using FDG-PET imaging. On the *x* and *y* axes, the first 2 discriminant functions, that is, the first 2 linear combinations of the regional values providing the best discrimination between the groups. Colored dots indicate individual data, by clinical diagnosis, that is, AD, LBD, PDD, FTD, and CBD. The squares indicate the group centroids.

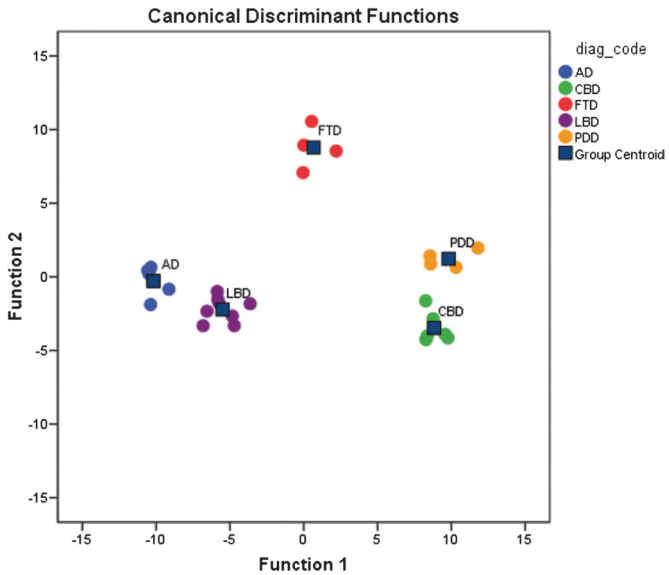

FIGURE 4. Two-dimensional projection plot of discriminant canonical functions for differentiation of patients with dementia using DAT and FDG-PET imaging. On the *x* and *y*, axes the first 2 discriminant functions, that is, the first 2 linear combinations of the regional values providing the best discrimination between the groups. Colored dots indicate individual data, by clinical diagnosis, that is, AD, LBD, PDD, FTD, and CBD. The squares indicate the group centroids.

both perfusion and DAT uptake ratios were taken into account, reaching an accuracy of 97.4%.[13]

In this retrospective study, we used an operator-independent, automated template-based discriminant analysis method to analyze both FDG-PET and DaTSCAN results for each patient. Our analysis focused specifically on its potential to distinguish AD, CBD, PDD, LBD, and FTD from each other. The main contribution of the use of an automated template-based approach is that the results of our analysis are unbiased and independent from the experience of the reader.

Interestingly, our results show that these 2 techniques, easily accessible in current clinical practice, allow a very good diagnostic precision when used together, with an overall accuracy of 88.9% in the cross-validation. More importantly, the information given by each of them is not redundant: only 51.9% of cross-validated grouped cases were correctly classified with DaTSCAN alone, and only 55.6% with normalized FDG uptake alone.

The method used in this work has been previously validated.[13] As in this previous work, we flipped the DAT data according to the clinically predominant affected side in case of asymmetric disease because there is a well-established correlation between the clinical expression and the most affected side. We did not flip the FDG-PET data to keep the information related to the functional lateralization of hemispheric functions, which might be relevant for differentiating neurodegenerative disorders.

To minimize the risk of false-positive results, the pretest likelihood was not based on the clinical picture, and all groups were set as equally probable in the discriminant analysis. When taking this information into account or adjusting the a priori likelihood of, for example, a distribution more related to clinical prevalence, age, and additional clinical parameters, the overall accuracy of this technique may further improve.

Care was taken here to provide also cross-validated results as a more unbiased predictor for future novel cases because it is well known that discriminant analysis without cross-validation can yield overly optimistic discrimination values.[26]

Importantly, the results of our analysis of FDG-PET data showed that the specific regions allowing the automatic classification of subjects in the different diagnostic groups are indeed the cortical and subcortical regions that have been described as typically affected in the various pathological entities. Indeed, they include the parietal cortex (PD and AD), the precuneus and the hippocampus (AD), the occipital cortex (LBD), and the thalami, the putamen, and the precentral cortex (CBD, FTD, PD).

The laterality of these findings, however, is more difficult to interpret: it might be due to a specific lateralization associated with the different degenerative syndromes but might also be specific for our sample of subjects.

The methods used in this work could be readily applied in a clinical setting: each center should select a sample of patients with a clinical diagnosis confirmed by follow-up, as in our case, and use it as "training set" to identify the regions, which allow the best discrimination among groups, which might vary across scanners and imaging protocols.

Each incoming patient could then be evaluated, in analogy with the cross-validation procedure we used: the program would provide the attribution to a diagnostic group with a given probability, and this information could support image interpretation and clinical workup.

For those centers not having the possibility to test discriminant analysis in-house because of a limited number of patients with defined clinical diagnoses or without access to the software tools needed to implement a platform of analyses, these results highlight some regions playing a more relevant role than others in the differential diagnosis of neurodegenerative syndromes. When visually reading the DAT images, the most affected putamen will be the first sign of a neurodegeneration of the nigrostriatal pathway to look for, and when reading the FDG-PET images, the precuneus will be the first cortical region to assess, given its early and specific involvement in AD cases.[29]

Study Limitations

This study has a few limitations that should be mentioned. First, the retrospective design, explaining the inhomogeneity of the subjects sample and the small number of subjects included, limits our ability to generalize these findings. In addition, clinical diagnosis was not blinded to the results of neuroimaging studies, adding a potential bias.

We had access to a limited number of patients compared with the larger number of independent variables that were analyzed (>20 regions of interest per hemisphere of the brain for FDG and 4 for ioflupane), which is a limitation, to apply a discriminant analysis. In fact, it is often preferred that at least 10 observations are used for each independent variable to properly predict the dependent variables of categorization, but we preferred not selecting the regions a priori, considering that this is an exploratory study. In the interpretation of functional neuroimaging data, multiple factors such as compensatory mechanisms or effects themselves of the medication might have an impact on the results. We have not included potential variables such as disease duration and the nature and the posology of various medications that our patients may have taken. However, this corresponds more closely to the usual patients' conditions in a clinical setting, and there are very few medications known to interfere with DAT imaging.

No neuropathological confirmation of the clinical diagnosis was available. It can thus be expected that a proportion of cases can be misclassified with respect to pathologic diagnosis.[30,31] However, in the absence of anatomopathologic confirmation, the canonical discriminant functions derived from this work lead to a diagnostic accuracy that is comparable to a high standard clinical evaluation and provide an objective, operator-independent classification in early the stage of the disease.

Finally, atrophy was not taken into account, given that not all subjects had a 3-dimensional T1-weighted MRI allowing a correction for partial volume effect. However, this is in line with most of the previous works investigating FDG-PET patterns in dementia diagnosis.

CONCLUSIONS

These preliminary results obtained by an automated approach suggest that the information obtained from the analysis of the normalized FDG uptake and DAT uptake ratios is not redundant in a sample of patients experiencing various neurodegenerative conditions. In fact, taking into account both approaches allows a better classification of each patient and a larger gain for the cross-validated cases.

Our results provide additional evidence of the value of functional brain imaging in the evaluation of complex neurodegenerative disorders. Why certain diseases affect some parts of the brain more than others is poorly understood, but analyses of functional patterns in these patients are important. These results also illustrate that the systematic investigation of both normalized FDG uptake and DAT uptake for these patients is justified, although unfortunately at a greater expense and inconvenience to the patient.

The automated technique we propose could be validated in larger and independent samples and may increase confidence to diagnose neurodegenerative disorders at an early stage.

Large databases for imaging studies performed in normal subjects, as well as in various diagnostic entities, are becoming increasingly available on an open-access basis.[24] In parallel, shared analysis platforms are under development, such as in the neuGRID (www.neuGRID.eu) and DECIDE (https://www.eu-decide.eu/) projects. In this perspective, it is of special interest to develop and to adapt automated tools able to combine various biomarkers for the "biochemical classification" of neurodegenerative disorders.

REFERENCES

1. Brooks DJ, Pavese N. Imaging biomarkers in Parkinson's disease. *Prog Neurobiol*. 2011;95:614–628.
2. Varrone A, Halldin C. Molecular imaging of the dopamine transporter. *J Nucl Med*. 2010;51:1331–1334.
3. McKeith I, O'Brien J, Walker Z, et al. Sensitivity and specificity of dopamine transporter imaging with ^{123}I-FP-CIT SPECT in dementia with Lewy bodies: a phase III, multicentre study. *Lancet Neurol*. 2007;6:305–313.
4. Antonini A, Benti R, De Notaris R, et al. 123I-Ioflupane/SPECT binding to striatal dopamine transporter (DAT) uptake in patients with Parkinson's disease, multiple system atrophy, and progressive supranuclear palsy. *Neurol Sci*. 2003;24:149–150.
5. Pirker W, Asenbaum S, Bencsits G, et al. [123I]beta-CIT SPECT in multiple system atrophy, progressive supranuclear palsy, and corticobasal degeneration. *Mov Disord*. 2000;15:1158–1167.
6. Cummings JL, Henchcliffe C, Schaier S, et al. The role of dopaminergic imaging in patients with symptoms of dopaminergic system neurodegeneration. *Brain*. 2011;134:3146–3166.
7. Bosman T, Van Laere K, Santens P. Anatomically standardised ^{99m}Tc-ECD brain perfusion SPET allows accurate differentiation between healthy volunteers, multiple system atrophy and idiopathic Parkinson's disease. *Eur J Nucl Med Mol Imaging*. 2003;30:16–24.
8. Lim SM, Katsifis A, Villemagne VL, et al. The ^{18}F-FDG PET cingulate island sign and comparison to ^{123}I-beta-CIT SPECT for diagnosis of dementia with Lewy bodies. *J Nucl Med*. 2009;50:1638–1645.
9. Foster NL, Heidebrink JL, Clark CM, et al. FDG-PET improves accuracy in distinguishing frontotemporal dementia and Alzheimer's disease. *Brain*. 2007; 130:2616–2635.
10. Eckert T, Barnes A, Dhawan V, et al. FDG PET in the differential diagnosis of parkinsonian disorders. *Neuroimage*. 2005;26:912–921.
11. Berti V, Polito C, Ramat S, et al. Brain metabolic correlates of dopaminergic degeneration in de novo idiopathic Parkinson's disease. *Eur J Nucl Med Mol Imaging*. 2010;37:537–544.
12. Klaffke S, Kuhn AA, Plotkin M, et al. Dopamine transporters, D2 receptors, and glucose metabolism in corticobasal degeneration. *Mov Disord*. 2006; 21:1724–1727.
13. Van Laere K, Casteels C, De Ceuninck L, et al. Dual-tracer dopamine transporter and perfusion SPECT in differential diagnosis of parkinsonism using template-based discriminant analysis. *J Nucl Med*. 2006;47:384–392.
14. McKeith IG, Galasko D, Kosaka K, et al. Consensus guidelines for the clinical and pathologic diagnosis of dementia with Lewy bodies (DLB): report of the consortium on DLB international workshop. *Neurology*. 1996;47:1113–1124.
15. McKhann G, Drachman D, Folstein M, et al. Clinical diagnosis of Alzheimer's disease: report of the NINCDS-ADRDA Work Group under the auspices of Department of Health and Human Services Task Force on Alzheimer's Disease. *Neurology*. 1984;34:939–944.
16. Hughes AJ, Daniel SE, Kilford L, et al. Accuracy of clinical diagnosis of idiopathic Parkinson's disease: a clinico-pathological study of 100 cases. *J Neurol Neurosurg Psychiatry*. 1992;55:181–184.
17. Neary D, Snowden JS, Gustafson L, et al. Frontotemporal lobar degeneration: a consensus on clinical diagnostic criteria. *Neurology*. 1998;51:1546–1554.
18. Riley DE, Lang AE, Lewis A, et al. Cortical-basal ganglionic degeneration. *Neurology*. 1990;40:1203–1212.
19. Slomka PJ, Radau PE, Hurwitz G, et al. Automated three-dimensional quantifi cation of myocardial perfusion and brain SPECT. *Comput Med Imaging Graph*. 2001;25:153–164.
20. Radau PE, Slomka PJ, Julin P, et al. Evaluation of linear registration algorithms for brain SPECT and the errors due to hypoperfusion lesions. *J Med Phys*. 2001;28:1660–1668.
21. Koch W, Radau PE, Hamann C, et al. Clinical testing of an optimized software solution for an automated, observer-independent evaluation of dopamine transporter SPECT studies. *J Nucl Med*. 2005;46:1109–1118.
22. Morton RJ, Guy MJ, Clauss R, et al. Comparison of different methods of DatSCAN quantification. *Nucl Med Commun*. 2005;26:1139–1146.
23. Efron B. Estimating the error rate of a prediction rule: improvements on cross-validation. *J Am Stat Assoc*. 1983;78:316–331.
24. Herholz K. PET studies in dementia. *Ann Nucl Med*. 2003;17:79–89.
25. Zhao P, Zhang B, Gao S. 18[F]-FDG PET study on the idiopathic Parkinson's disease from several parkinsonian-plus syndromes. *Parkinsonism Relat Disord*. 2012;18(suppl 1):S60–S62.
26. Charpentier P, Lavenu I, Defebvre L, et al. Alzheimer's disease and frontotemporal dementia are differentiated by discriminant analysis applied to (99m)Tc HmPAO SPECT data. *J Neurol Neurosurg Psychiatry*. 2000;69:661–663.
27. Kreisler A, Defebvre L, Lecouffe P, et al. Corticobasal degeneration and Parkinson's disease assessed by HmPaO SPECT: the utility of factorial discriminant analysis. *Mov Disord*. 2005;20:1431–1438.
28. Spetsieris PG, Ma Y, Dhawan V, et al. Differential diagnosis of parkinsonian syndromes using PCA-based functional imaging features. *Neuroimage*. 2009; 45:1241–1252.
29. Herholz K, Carter SF, Jones M. Positron emission tomography imaging in dementia. *Br J Radiol*. 2007;80:S160–S167.
30. Mok W, Chow TW, Zheng L, et al. Clinicopathological concordance of dementia diagnoses by community versus tertiary care clinicians. *Am J Alzheimers Dis Other Demen*. 2004;19:161–165.
31. Piguet O, Halliday GM, Creasey H, et al. Frontotemporal dementia and dementia with Lewy bodies in a case-control study of Alzheimer's disease. *Int Psychogeriatr*. 2009;21:688–695.